



TITLE:

Polarization and intensity of Compton scattering

AUTHOR(S):

Saito, Naoki; Tanaka, Ryohei; Kawai, Jun

CITATION:

Saito, Naoki ...[et al]. Polarization and intensity of Compton scattering. X-Ray Spectrometry 2022, 51(1): 86-90

ISSUE DATE:

2022-01

URL:

<http://hdl.handle.net/2433/278979>

RIGHT:

© 2021 The Authors. X-Ray Spectrometry published by John Wiley & Sons Ltd.; This is an open access article under the terms of the Creative Commons Attribution-NonCommercial License, which permits use, distribution and reproduction in any medium, provided the original work is properly cited and is not used for commercial purposes.

Polarization and intensity of Compton scattering

Naoki Saito | Ryohei Tanaka  | Jun Kawai 

Department of Materials Science and Engineering, Kyoto University, Kyoto, Japan

Correspondence

Jun Kawai, Department of Materials Science and Engineering, Kyoto University, Sakyo-ku, Kyoto 606-8501, Japan.

Email: kawai.jun.3x@kyoto-u.ac.jp

The copyright line for this article was changed on 17 December 2021 after original online publication.

X-ray spectra scattered at 90° by acrylic resin plates of various thicknesses are measured. The intensity and polarization of Compton-scattered X-rays are estimated from the spectra. As the thickness of the slab increases, the intensity increases but the polarization decreases. The optimal thickness for a polarized X-ray fluorescence spectrometer is determined, which provides both high intensity and high polarization.

KEYWORDS

Doppler effect, polarization XRF, polarized X-rays, white X-ray polarization

1 | INTRODUCTION

Compton scattering is usually believed as an incoherent scattering. However, Schrödinger¹ interpreted the Compton scattering as a Bragg diffraction of incident X-rays by a periodic de Broglie wave of the scattered Compton electron. The Bragg diffraction is a coherent scattering due to the interference between the incident and scattered X-rays in a crystal's periodic electron density. The Compton-scattered X-rays are also interfered with the incident X-rays within the electron density lattice of the de Broglie wave packet. The de Broglie electron travels by a group velocity of say 10% of the speed of light, and thus the Compton-scattered X-rays are Doppler-shifted. The group velocity of a free electron is p/m , whereas the phase velocity is $p/(2m)$, where m and p are respectively the electron mass and its momentum. The Brewster's angle of the X-rays is 45° , and thus the 90° Bragg-diffracted X-rays have theoretically perfect polarization.

Some believe that Compton scattering is not Barkla scattering, and some knows Compton scattering is a kind of coherent scattering after the interpretation of Schrödinger.¹ Barkla² used blocks of carbon to produce the scattering,³ and thus the Barkla scattering was the

Compton scattering. Barkla observed the polarization in 90° Compton scattering.

Champion et al.⁴ made a polarized X-ray fluorescence (XRF) spectrometer using a topaz single crystal as a polarizer using the 45° Bragg diffraction. Based on the wave picture of the Compton scattering by Schrödinger,¹ Tanaka and Kawai⁵ calculated the phase velocity of de Broglie wave and the Compton energy shift when the incident X-rays are scattered at the 90° direction. Based on this calculation, Tanaka et al.⁶ generated highly polarized continuous X-rays using a scattering object composed of low atomic number elements, such as acrylic resin, by 90° Compton scattering. The comparison of 90° polarization between acryl $(C_5H_8O_2)_n$ and lead (Pb) plates was reported by Yamashita et al.⁷

In 1991 Robertson⁸ already submitted a patent of using 115 keV Bremsstrahlung polarized X-rays in order to analyze up to uranium elements in ore by high energy K line XRF. Zhalsaraev⁹ evaluated the effects of polarized X-rays for the sensitivity and detection limits of wavelength-dispersive¹⁰ and energy-dispersive¹¹ XRF spectrometers.

From previous papers⁵⁻⁷ of the present authors' group, an acrylic plate or acrylic slab is considered a good

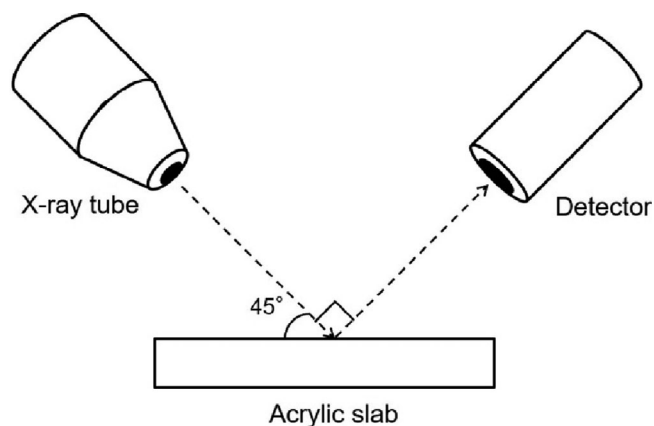


FIGURE 1 Experimental setup for the measurements of the X-ray spectra scattered at 90° from acrylic slabs of 2–20 mm thicknesses

candidate for X-ray polarizer; the present paper reports the thickness dependence of both the polarization and Compton profiles from Rh tube X-rays. The optimum condition, which provides both high intensity and high polarization for XRF spectrometer, is reported.

2 | EXPERIMENTAL

Figure 1 shows the setup for the measurements of the X-ray spectra (Figure 3 below) scattered at 90° from acrylic slabs of 2–20 mm thicknesses. The angle among the X-ray tube, acrylic plates, and detector was set at 90° . Table 1 shows the experimental apparatus and parameters. The X-ray tube and detector were the same as those used by Tanaka et al.⁶

Figure 2 shows the spectrometer used to measure the polarization of scattered X-rays from acrylic plates. It is somewhat similar to the one made by Yamashita et al.⁷ The X-ray tube, acrylic slabs, scatterer (a 5 mm thick acrylic plate), and the detector are arranged as shown in Figure 2(a). The glancing angle between the incident horizontal X-rays and the surface of the first slab was 45° ; the X-rays were vertically (z -axis) scattered upward and then scattered again by a scatterer to a horizontal direction. Figure 2(b)–(e) shows holders made of polylactic acid (PLA) using a 3D printer. As shown in Figure 2(d), (e), the holders could vary the azimuthal angle ϕ every 30° in the x – y plane in Figure 2(a). ϕ was defined as the angle between the directions of the incident X-rays and the X-rays scattered by the scatterer. The acrylic plates and the scatterer were attached to the X-ray tube holder and the detector holder. A lead (Pb) collimator with a 2 mm diameter hole was attached to the detector window.

TABLE 1 Experimental conditions

X-ray tube	Moxtek
	Ultra-lite magnum
	Rhodium anode
	Max power (for present report): 30 kV, 4 W
Detector	SDD: KETEK
	Electric circuit: RES lab (Osaka)
	Measured duration: 100–1,000 seconds
Polarizer	Acryl resin plate ($C_5O_2H_8$) _n
	Thickness: from 2 to 20 mm
	Density: 1.18 g/cm ³

3 | RESULTS AND DISCUSSION

Figure 3 shows the X-ray spectra scattered at 90° from the acrylic slabs from 2 to 20 mm thicknesses. It is found from Figure 3 that the Compton intensity of Rh $K\alpha$ increased with the increase in thickness. That is to say, the Compton peak intensity (integral intensity) increased from 340 cps (2 mm) to 900 cps (20 mm). The intensity of X-rays scattered when they pass through the material is proportional to $1 - \exp(-\rho\mu d)$, where ρ is the density of material, μ the mass-attenuation coefficient, and d the pass length. Therefore, as the thickness (d) increased, the scattered X-ray intensity also increased. Figure 4 shows the thickness dependence of the intensity of Rh $K\alpha$ Compton peak. It is understood from Figure 4 that the intensity increases as a function of $1 - \exp(-\rho\mu d)$.

The polarization of the scattered X-rays at 90° from acrylic plates was measured. The polarization was defined as the ratio of an amplitude of a modulation curve to the average of scattered X-ray intensity, $\frac{N_{\parallel} - N_{\perp}}{N_{\parallel} + N_{\perp}}$. Here, N_{\parallel} and N_{\perp} denote the intensity of scattered X-rays as the detection angle is parallel ($\phi = 0^\circ$ as shown in Figure 2(d)) and perpendicular ($\phi = 90^\circ$ as shown in Figure 2(e)) to the direction of the incident X-rays. Polarization is 0 for unpolarized X-rays and 1 for perfectly polarized X-rays. Figure 5 shows the measured angular dependence of the Rh $K\alpha$ Compton intensity scattered from the acrylic slabs of 2 and 20 mm thicknesses. To compare the polarization, the $\cos \phi$ fitted curves were normalized with respect to the intensities at 90° . As the thickness of the slabs decreased from 20 to 2 mm, the polarization of Rh $K\alpha$ Compton increased from 0.56 (20 mm) to 0.62 (2 mm). The polarizations from 2 to 20 mm thicknesses of the slabs are plotted in Figure 4. It is found from Figure 4 that the decrease in the thickness of the slabs led to the increase in polarization.

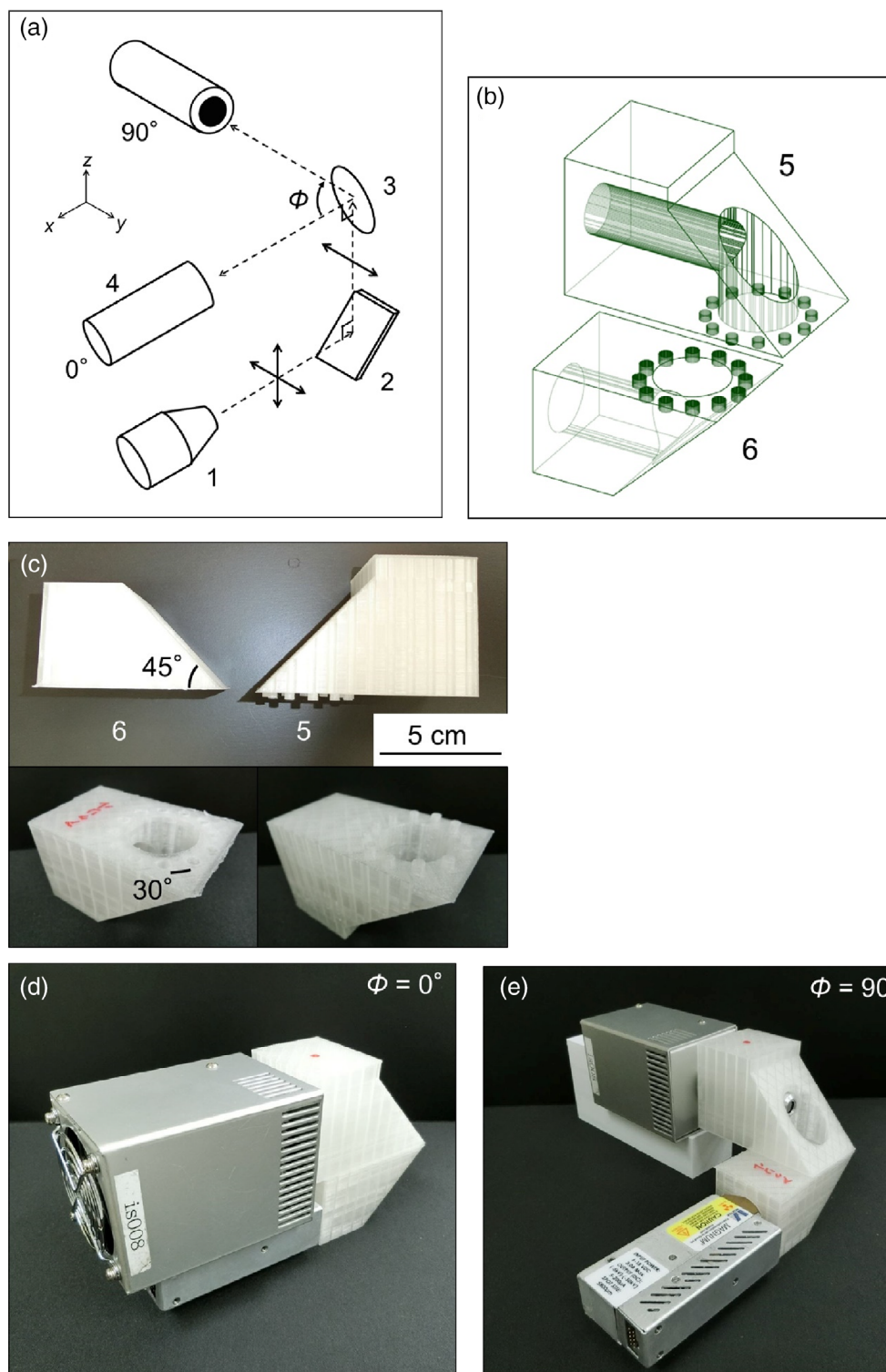


FIGURE 2 Spectrometer with the use of a 3D printer to measure the polarization of scattered X-rays from acrylic plates. (a) Experimental setup, (b) 3D CAD models of holders, (c) holders (holes and ticks are at 30° interval), (d) spectrometer at $\phi = 0^\circ$, and (e) $\phi = 90^\circ$. 1: X-ray tube, 2: acrylic resin plate, 3: scatterer (thin acrylic resin), 4: detector, 5: detector holder, and 6: X-ray tube holder [Colour figure can be viewed at wileyonlinelibrary.com]

Figure 6 shows the enlarged spectra around the Compton peak for both 2 and 20 mm thicknesses in Figure 3. They were normalized with respect to the maximum intensity of Rh $K\alpha$ Compton peak here. It is found from Figure 6 that the Rh $K\alpha$ Compton peak was broadened to the lower energy side by increasing the thickness.

The energy shift E' of Compton scattering as the change of the scattering angle θ is expressed by

$$E' = \frac{E}{1 + \frac{E}{mc^2}(1 - \cos\theta)}, \quad (1)$$

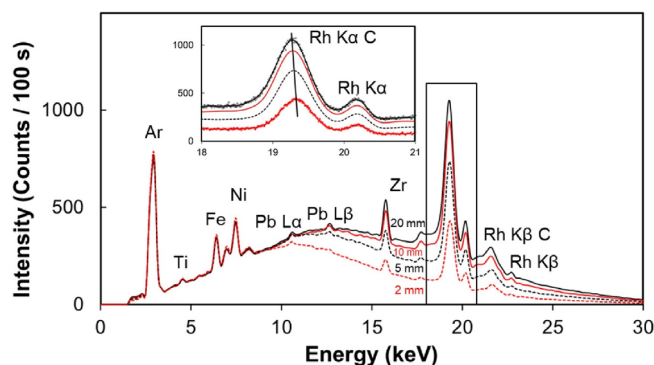


FIGURE 3 X-ray spectra scattered at 90° from acrylic slabs of different thicknesses. Compton peaks are denoted by C. The tube power was 30 kV and 5.0 μA. Inset is the enlarged spectra of the box between 18 and 21 keV. Minor peaks are Fe Kβ (7.1 keV), Ni Kβ (8.3 keV), and Zr Kβ (17.7 keV) [Colour figure can be viewed at wileyonlinelibrary.com]

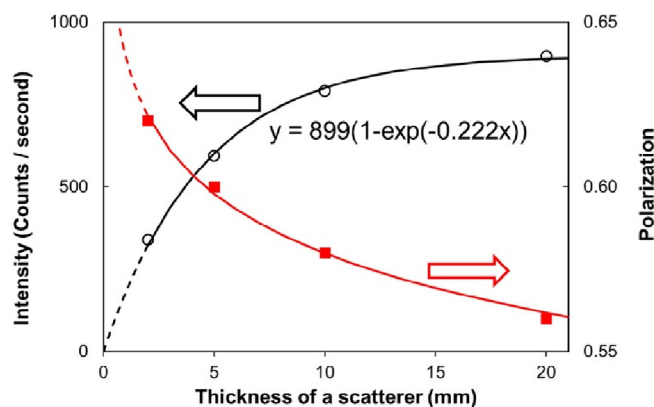


FIGURE 4 The thickness dependence of the integrated intensity and polarization within the energy range of Rh Kα Compton. Black dots (measured) and line (fitted) are for intensity, and red ones are for polarization. The polarization curve (red) is for guiding the reader's eye, but the profile is approximately symmetric to the intensity exponential curve [Colour figure can be viewed at wileyonlinelibrary.com]

where E is the energy of the incident X-ray, m the electron mass, and c the speed of light. When the thickness of the slab increased, the X-ray scattering angle changed, as shown in Figure 7. The increase of thickness means widening of the effective scattering angles. The energy positions of the broken vertical lines in Figure 6 indicate the energy of the Rh Kα Compton peak scattered by the 20 mm thick slab, but the depth is at 0, 2, 5, and 10 mm from the surface. The surface of the slab was 45° incident and 90° scattered X-rays (the dashed vertical line “a” in Figure 6), estimated from Equation (1). Figure 6 shows the increase of intensity broadened the Compton peak. The polarization is expressed as $\frac{1 - \cos^2\theta}{1 + \cos^2\theta}$, where θ is the

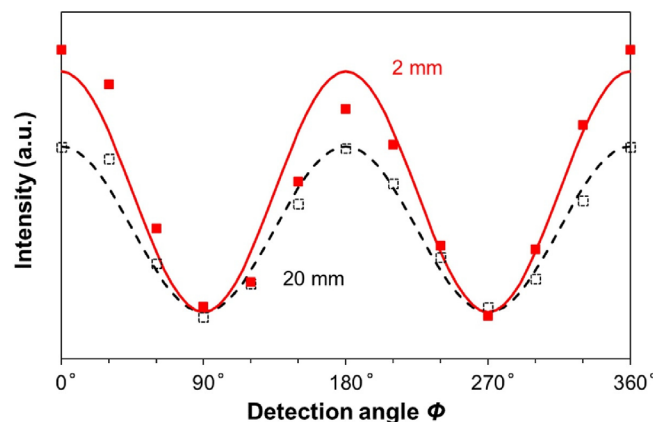


FIGURE 5 The angular dependence of the X-ray (Rh Kα Compton) intensity scattered from the acrylic slabs of different thicknesses. Solid dots (measured) and line (Cosine curves are least square fitted to the measured intensity.) are for 2 mm, and broken ones are for 20 mm [Colour figure can be viewed at wileyonlinelibrary.com]

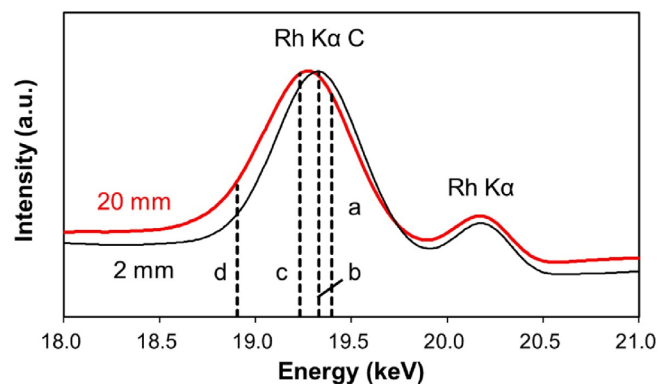


FIGURE 6 The broadening of the Rh Kα Compton peak with increasing thickness of the acrylic slab. Calculated Compton scattered peak energy at (a) depth 0, (b) 2, (c) 5, and (d) 20 mm by using Equation (1), where θ is defined by Figure 7 [Colour figure can be viewed at wileyonlinelibrary.com]

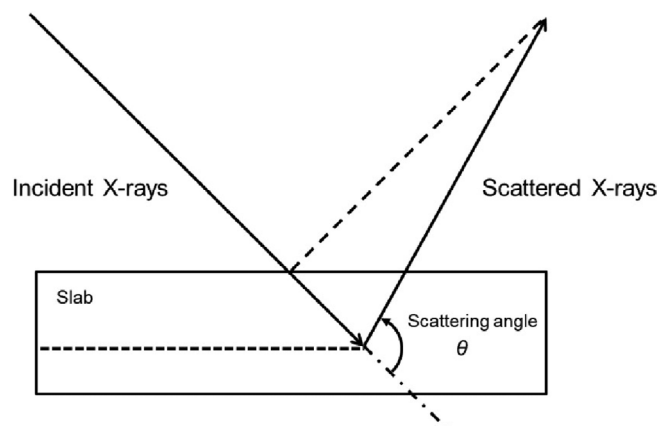


FIGURE 7 Relation between the thickness and the X-ray scattering angle

scattering angle. The polarization is unity at $\theta = 90^\circ$. When θ is larger than 90° , it decreases. Therefore, the increase in the thickness of the acrylic slabs caused the decrease in polarization.

4 | CONCLUSIONS

X-ray spectra scattered at 90° were measured. X-rays emitted from the Rh X-ray tube (30 kV, 4 W) were scattered from slabs of 2–20 mm thick acrylic resin ($C_5H_8O_2$)_n in the air. The intensity and polarization of the scattered X-rays were measured. The results obtained in the present study were summarized as follows.

As the thickness of the slabs increased from 2 mm to 20 mm:

1. The integrated intensity within the energy range of Rh $K\alpha$ Compton increased from 340 cps (2 mm) to 900 cps (20 mm).
2. The polarization within the same energy range decreased from 0.62 (2 mm) to 0.56 (20 mm). Here the polarization is defined as zero for unpolarized X-rays and unity for perfectly polarized X-rays.

In conclusion, the slab of acrylic resin with a thickness of ~ 10 mm is suitable (optimal) for a polarizer of XRF spectrometer with a low-power X-ray source.

It should be noted that the X-ray polarization is quite easily observable through a spectrometer made of 3D printed parts.

The Schrödinger's interpretation¹ is quite important that the Compton scattering is not an incoherent scattering, but a kind of coherent scattering phenomenon even though the incident and scattered X-ray wavelengths are different; the Compton scattering is a kind of Bragg diffraction by high-speed Compton

electron, which has a periodic de Broglie wavelength; thus, the Compton scattering is a kind of Doppler effect.

DATA AVAILABILITY STATEMENT

Data derived from public domain resources.

ORCID

Ryohei Tanaka  <https://orcid.org/0000-0002-7517-1635>

Jun Kawai  <https://orcid.org/0000-0002-1289-7666>

REFERENCES

- [1] E. Schrödinger, *Ann Phys* **1927**, 387, 257. <https://doi.org/10.1002/andp.19273870210>
- [2] C. G. Barkla, *Proc Royal Soc* **1906**, A77, 247. <http://doi.org/10.1098/rspa.1906.0021>
- [3] A. H. Compton, S. K. Allison, *X-rays in theory and experiment*, 2nd ed., Van Nostrand, Princeton, NJ **1926**, 1954, 1935, p. 19.
- [4] K. P. Champion, R. N. Whittam, *Nature* **1963**, 199, 1082. <https://doi.org/10.1038/1991082a0>
- [5] R. Tanaka, J. Kawai, *Adv X-Ray Chem Anal Japan* **2018**, 49, 189. <https://www.researchgate.net/publication/324368579>
- [6] R. Tanaka, T. Sugino, D. Yamashita, N. Shimura, J. Kawai, *Anal Kontrol* **2018**, 22, 128. <https://doi.org/10.15826/analitika.2018.22.2.010>
- [7] D. Yamashita, R. Tanaka, J. Kawai, *Adv X-Ray Chem Anal Japan* **2021**, 52, 49. <https://www.researchgate.net/publication/350790312>
- [8] M. E. A. Robertson, *US Patent 5,020,084*. **May 28, 1991**. <https://pdfpiw.uspto.gov/.piw?PageNum=0&docid=05020084>
- [9] B. Z. Zhalsaraev, *X-Ray Spectrometry* **2019**, 48, 628. <https://doi.org/10.1002/xrs.3046>
- [10] B. Z. Zhalsaraev, *X-Ray Spectrometry* **2020**, 49, 480. <https://doi.org/10.1002/xrs.3142>
- [11] B. Z. Zhalsaraev, *X-Ray Spectrometry* **2021**, 50, 28. <https://doi.org/10.1002/xrs.3187>

How to cite this article: N. Saito, R. Tanaka, J. Kawai, *X-Ray Spectrom* **2022**, 51(1), 86. <https://doi.org/10.1002/xrs.3261>